JOURNAL OF CATALYSIS 27, 64–69 (1972)

Strain Energy Considerations in the Effect of a Class of Catalyst Promoters

J. M. SCHULTZ

Department of Chemical Engineering, University of Delaware, Newark, Delaware 19711

Received January 20, 1972

It is shown that the crystallite size refining and maintaining phenomena evidenced by the singly promoted ammonia catalyst can be attributed to a delicate balance between strain energy and surface energy effects. In the model presented the promotor acts as the point defect source of a strain field. The strain field of the point defects can be partially relaxed by the propinquity of a free surface. This comminuting effect is resisted by the creation of free surface. It is shown that for a certain narrow range of material parameters the strain and surface terms achieve a balance which produces an equilibrium particle size. It is shown, finally, that the material parameters of the alumina-promoted iron catalyst lie in a range in which the strain-surface energy effect is feasible.

There exists a class of catalyst promoter, typified by the alumina-promoted iron catalyst for ammonia synthesis, which appears to be effective in producing and maintaining a fine particle size, vis-à-vis enhancing the specific activity of the surface. It is common, in discussing such materials, to state that the promoter resides at or near the surface of the catalyst particle and inhibits thereby the sintering of adjacent particles. This type of description is vague and does not really define the physics (or chemistry) by which coalescence of particles is hindered. In the present paper an attempt is made to define the nature of the sintering inhibition.

Before proceeding to a description of the attack used here, it is useful to very briefly describe the processing of the catalyst and to enumerate a few of the structural details observed in the final product. The type of catalyst treated here is typically produced by the reduction of a mixed oxide. The oxide is generally dilute in the promoting agent, e.g., an iron–aluminum spinel with an Al_2O_3 content of some few percent. The following are some of the specific characteristics of the reduced FeAl spinel ammonia synthesis catalyst.

1. The initial specific activities of promoted and unpromoted reduced oxide are the same. However, the activity of the unpromoted catalyst drops rapidly with reaction time, relative to the promoted material (*1*).

2. Promotion by alumina is effective only when the alumina is homogeneously distributed in the iron oxide matrix prior to reduction (*1*, *2*).

3. The solubility of alumina in the reduced spinel is about 3%. Excess alumina precipitates out as thin particles separating iron grains (*3*).

4. The activity of the singly promoted catalyst varies with alumina content and peaks at some 3% alumina (*4*).

5. The Al exists in the reduced iron matrix as homogeneously distributed $FeAl_2O_4$ point defects (*5*). These defects have a diameter about 6.3% too large for the sites they occupy and thereby cause a measurable and severe distortion of the matrix.

6. The crystallite size of the promoted, reduced catalyst is in the range 200–500 Å (*5–7*).

7. X-Ray line broadening studies show that the small crystallite size of the reduced catalyst is imparted with the reduction event and remains constant thereafter (*7*).

Any explanation of the effect of Al_2O_3 on the ammonia catalyst must be consistent with these observations. Indeed, it is possible that such an explanation would have implications extending to Fischer-Tropf catalysts and other reduced oxide catalytic materials.

The model presented here may be seen in the following way. It is clear from the work of Hosemann, Preisinger, and Vogel (*5*) that the alumina promoter in the reduced iron catalyst exists as well-distributed point defects and that these defects exert an enormous disruptive influence on the crystalline iron matrix. We envision the elastic nature of the point defect as in Fig. 1. In this we consider placing a small, hard sphere of radius r_0 into a spherical hole of radius $r'_0 < r_0$ within a softer matrix material. In order to compute the elastic fields set up in fitting the large, hard sphere into the hole, we consider a pressure p to be appiled to the periphery of the hole to expand it to radius r_0. Finally the sphere is placed in the hole. If the sphere is much harder than the matrix, no relaxation of the matrix will occur and a radially directed stress of magnitude $\sigma_{rr}(r_0) = -p$ acts at the interface between the sphere and the matrix. Thus a stress field of magnitude $\sigma_{rr}(r)$ is generated within the solid. A considerable energy is stored in this stress field. Now the stress field can be shown to be proportional to r^{-3} (see Appendix). Surfaces of constant stress level will be as depicted schematically in Fig. 2. Suppose the solid were now divided physically into two parts, as shown in Fig. 2, a sphere of radius R containing the defect and the remainder. The two portions are not in contact; their former interface is replaced by two (adjacent) free surfaces. The total amount of energy stored can thereby be lowered (relative to the larger piece) because the outer portion of the strain field now no longer exists. If only this effect were active, the new surface would be coincident with the particle–matrix interface, since maximum stress relief would be attained by removing the included particle entirely from the matrix. Indeed, this would be the case of phase separation. In our case, however, we presume the misfit to be not quite great enough to produce phase separation. We now note that the strain energy effect is constrained by a surface energy term of magnitude $4\pi R^2\gamma$, where γ is the surface free energy (erg/cm²). Thus there should be some stable particle radius R at which the strain energy term plus the surface energy term reach a minimum.

A similar situation should exist in a piece containing many stress-generating point defects. We might expect again a minimum energy particle size to exist. But now each

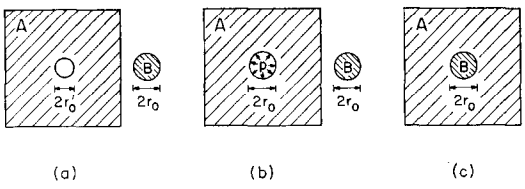

FIG. 1. Model for the calculation of elastic effects involved in the inclusion of a hard sphere defect in a relatively soft matrix: (a) separate soft matrix A (with spherical hole of radius r'_0) and hard sphere B of radius $r'_0 > r_0$; (b) expansion, by pressure p, to increase hole in matrix from radius r'_0 to radius r_0; (c) insertion of hard sphere into the expanded hole in the matrix.

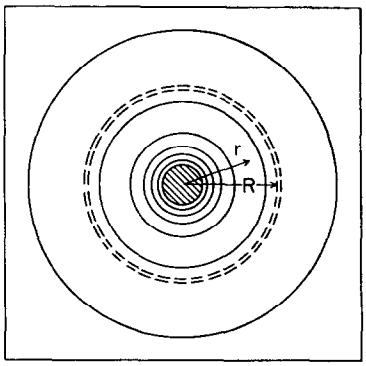

FIG. 2. Schematic iso-stress lines about a hard spherical defect. Double broken line indicates truncation of spherical crystallite at radius R.

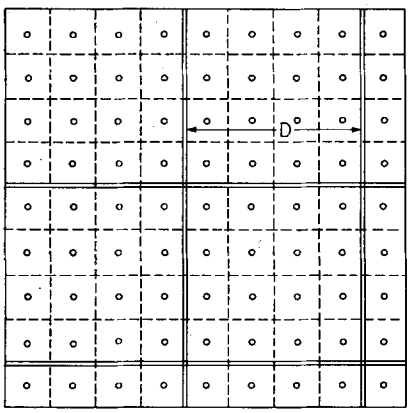

FIG. 3. Division into crystallites of breadth D for a material containing a homogeneous distribution of point defects.

particle could include several defects, as in Fig. 3. In this, each particle would contain several interior defects whose elastic fields are essentially complete, as well as defects near the free surface with the fields considerably relaxed. In the next section we assess the functionality between the breadth D of such regions and the physical parameters of the material.

ANALYSIS

It is not difficult to show that beyond a radius of some $R = 3r_0$ the energy of a sphere of radius R is not significantly different from the energy stored in a sphere of infinite extent. This exercise is performed in the Appendix. With this result we can get some idea as to the equilibrium particle size by considering a model in which all defects within some thin shell near the free surface are totally relaxed, whereas those below that shell maintain their entire elastic field. This is the situation idealized in Fig. 3 and in the subsequent algebra.

We consider here a solid separated into cubic crystallites of diameter D. These crystallites are fully separated from each other. As indicated above, we presume that any point defects whose centers lie within pr_0 (p = small integer) of the surface are fully relaxed. Surely this will be the case if $p = 1$; then the particle lies in the surface. The condition could possibly also be satisfied for $p = 2$ or $p = 3$, but no vehicle exists for calculating strain fields at the unit cell level. The model allows all defects not contained in the outer shell of thickness pr_0 to produce their full, infinite solid strain energy.

The energy stored per unit volume is calculated, on this model, in the following way. In the cubic crystallite of edge D and random defect concentration N defects per unit volume, the number of defects n_{eff} which contribute to the strain energy is

$$n_{\text{eff}} = (D - 2pr_0)^3 N. \tag{1}$$

The active, stress-promoting fraction f of all defects is then

$$f = \frac{n_{\text{eff}}}{D^3 N} = \frac{(D - 2pr_0)^3}{D^3} = 1 - 6pr_0 \frac{1}{D} + 12p^2 r_0^2 \frac{1}{D^2} - 8p^3 r_0^3 \frac{1}{D^3}. \tag{2}$$

For defects which contribute an energy E_d per defect the strain energy per unit volume E_s will be

$$E_s = fNE_d. \tag{3}$$

In addition, surface of area $12D^2$ (12, not 6, since two surfaces form for each "cut") and energy γ per unit area is created for each crystallite formed. The interfacial energy E_I stored per unit volume is thus

$$E_I = \frac{12D^2\gamma}{D^3} = \frac{12\gamma}{D}. \tag{4}$$

The total energy stored for a system composed of crystallites of width D is thus

$$E_T = E_s + E_I = \left(1 - 6pr_0 \frac{1}{D} + 12p^2 r_0^2 \frac{1}{D^2} - 8p^3 r_0^3 \frac{1}{D^3}\right) \times NE_d + \frac{12\gamma}{D}. \tag{5}$$

The condition for equilibrium of this system is that E_T be a minimum with respect to D ($\partial E_T/\partial D|_{D=D^*} = 0$). Thus,

$$0 = \left.\frac{\partial E_T}{\partial D}\right|_{D^*} = (6pr_0 NE_d - 12\gamma)\frac{1}{D^{*2}} - 24p^2 r_0^2 NE_d \frac{1}{D^{*3}} + 24p^3 r_0^3 NE_d \frac{1}{D^{*4}}. \tag{6}$$

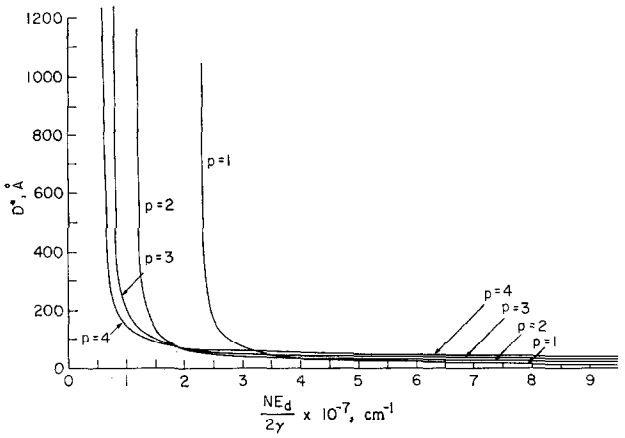

FIG. 4. Equilibrium crystallite size versus energy parameter $NE_d/2\gamma$.

Solving this quadratic algebraic equation for D^*, the equilibrium crystallite size, we find

$$D^* = \frac{2pr_0[1 \pm (2\gamma/pr_0NE_d)^{1/2}]}{1 - (2\gamma/pr_0NE_d)} \quad (7)$$

Figure 4 shows D^*, the equilibrium crystallite thickness plotted against $NE_d/2\gamma$ using $p = 1,2,3$, and 4.* In the computation a value of $r_0 = 4.5$ Å was used. This value is commensurate with the $FeAl_2O_4$ defect model proposed by Hosemann and Preisinger (*5*). Figure 4 demonstrates that for any reasonable value of p (representing the excluded layer thickness) D^* is not far different from $2pr_0$, the thickness of two excluded layers, unless $NE_d/2\gamma$ lies below some critical level. However, below this critical level the value of D^* begins a dramatic increase as $NE_d/2\gamma$ is lowered. The high $NE_d/2\gamma$ behavior represents a tendency toward phase segregation. The trend of D^* going to infinity as $NE_d/2\gamma$ approaches $(pr_0)^{-1}$ represents the other extreme, in which the strain energy term is always small compared with the surface energy contribution. The limiting case here represents the normal random solid solution behavior. But most importantly, we observe an intermediate region in which $NE_d/2\gamma$ is of the same order as $(pr_0)^{-1}$. In this size domain D^* is markedly affected by the explicit value of $NE_d/2\gamma$. This is the size domain in which the point defect content should produce a stable crystallite size.

The value of $NE_d/2\gamma$ for the optimal ammonia catalyst appears to fall in the proper regime for defect control. For this material appropriate values are as follows:

a. the weight fraction of Al_2O_3 in the material is about 3% (*3*);

b. the linear dilatation of the $FeAl_2O_4$ defect in the Fe lattice is about 6.25% (*5*);

c. $\mu = 8.6 \times 10^{11}$ dyne/cm^2 (*8*) and

d. $\gamma = 10^3$ erg/cm^2 [a value representative of solid–vapor surface energies (*9*)].

Using the 3 wt % value for the Al_2O_4 content, we find for N:

$$N\left(\frac{\text{defects}}{\text{cm}^3}\right) = \left(.03\,\frac{\text{g Al}_2\text{O}_3}{\text{g Fe}}\right)\left(7.87\,\frac{\text{g Fe}}{\text{cm}^3}\right) \times \left(\frac{1\text{ g mole Al}_2\text{O}_3}{8.6\text{ g Al}_2\text{O}_3}\right) \times \left(6.03 \times 10^{23}\,\frac{\text{Al}_2\text{O}_3\text{ molecules}}{\text{g mole Al}_2\text{O}_3}\right) = 1.65 \times 10^{21}\,\frac{\text{defects}}{\text{cm}^3}. \quad (8)$$

For E_d we use (A4) in the limit $R \to \infty$:

$$E_d = \frac{3\mu r_0^3}{2\pi^2}\left(\frac{\delta v}{r_0^3}\right)^2 = \frac{8}{3}\,\mu r_0^3\left(\frac{\delta v}{v}\right)^2, \quad (9)$$

where μ is the shear modulus and $\delta v/v$ is the volume dilation. In our case

* In the computation the + sign was used in the numerator. The − sign represents the case in which the point defect is sequestered by a free surface at its periphery.

$$E_d = \left(\frac{8}{3}\right)(8.6)(10)^{11}(4.5)^3(10)^{-24}(1.06^3 - 1)^2 = 8.36 \times 10^{-12}. \quad (10)$$

Multiplying (8) by (10) we find $NE_d/2\gamma = 0.7 \times 10^7$ erg/cm^3. This value is of the correct order of magnitude to produce a strain energy comminution effect (see, e.g., curves $p = 3$, $p = 4$ of Fig. 4). With the approximations involved in deriving (7) and with the numerical uncertainties in Fig. 4, it is impossible to do more than to demonstrate this feasibility.

Discussion

The thrust here has been to demonstrate that the equilibration of strain and surface effects results in a stable particle size under certain conditions. The particle is constrained by strain energy from growth and by surface energy from shrinking. The argument, however, rests upon the inability of the point defects to move to the surface of the crystallite. The results of Hosemann, Preisinger, and Vogel (*5*) indeed indicate that the defects remain distributed within the crystallites. Undoubtedly the large size of the $FeAl_2O_4$ defect renders it quite immobile in the Fe lattice. We would then envision the recrystallization which occurs during reduction to proceed via iron atom rearrangements about the immobile defects. Clearly, such a process requires an initial homogeneous distribution of cations in the spinel. It is unlikely that procedures which are much different from the reduction of mixed oxides would produce the proper homogeneity and immobility of the defect.

In general the above model satisfies all of the requirements set forth in the introduction:

1. There should be no difference in initial reactivity between promoted and unpromoted materials. The difference should occur with time as the unpromoted catalyst sinters.

2. The activity of the catalyst requires a high promoter concentration, but is not aided by concentrations so large that precipitation of the promoter occurs. Figure 4 shows that the maximum effect of promotion should be achieved for concentrations just below the solubility limit.

3. A homogeneous distribution of promoter and a large defect size are both essential to the comminution effect.

4. The crystallite size comminution should be coincident with the reduction process and should not change thereafter.

Finally, the comminution effect described here rests on a very delicate balance of proper values of material parameters (N, E_d, γ, μ, δv, r_0). While these considerations should lead toward rational engineering of new strain-comminuted materials, achieving a proper balance of material parameters will not reduce the arduousness of the task.

Appendix. Elastic Field About an Included Defect

The radially directed displacement field u_r about the defect is related to the radial position r, the volume δv displaced by the defect sphere, the shear and bulk moduli, μ and λ, of the matrix, and the radius R of the crystallite through (*10*)

$$u_r = \frac{\delta v}{4\pi r^2} + \alpha r, \quad \alpha = \frac{4\mu}{2\mu + 3\lambda}\left(\frac{\delta v}{4\pi R^3}\right). \quad (A1)$$

From the displacement field the radial strain and stress fields, ϵ_{rr} and σ'_{rr} are written

$$\epsilon_{rr} = \frac{\partial u_r}{\partial r} = \frac{\delta v}{4\pi}\left(-\frac{2}{r^3} + 0.643\,\frac{1}{R^3}\right), \quad (A2)$$

$$\sigma_{rr} = (\lambda + 2\mu)\frac{\partial u_r}{\partial r} + \frac{2\lambda u_r}{r} = \frac{\mu \delta v}{\pi}\left(\frac{1}{R^3} - \frac{1}{r^3}\right). \quad (A3)$$

In (A2) we have substituted values of μ and λ which are appropriate for α-iron ($\mu = 8.6 \times 10^{11}$ dyne/cm^2, $\lambda = 12.1 \times 10^{11}$ dyne/cm^2). The total energy stored in the sphere is thus

$$E_R = \int_{r_0}^{R} (4\pi r^2 \sigma_{rr})\epsilon_{rr} dr = \frac{\mu(\delta v)^2}{2\pi^2 r_0^3} \times \left[-2.357\left(\frac{r_0}{R}\right)^3 + 3 - 1.32\left(\frac{r_0}{R}\right)^3 \times \ln\frac{R}{r_0} - 0.643\left(\frac{r_0}{R}\right)^6\right]. \quad (A4)$$

According to this result of classical elas-

ticity, the strain energy contained in a sphere of radius $R = 2r_0$ is 13% less than that contained in an infinite solid, while the energy contained in spheres of $3r_0$ and $4r_0$ are 4 and 2% of the infinite solid value. Clearly classical elasticity will not have quantitative meaning at this unit cell size level. Nevertheless we may safely conclude that *the defect must exist immediately adjacent to a free surface if its strain energy contribution is to be significantly lowered.*

Acknowledgments

The author gratefully acknowledges productive discussions with Dr. G. C. A. Schuit and Professor E. Ruckenstein.

References

1. Mittasch, A., and Keunecke, E., *Z. Elektrochem.* **38**, 666 (1932).
2. Brill, R., *Z. Elektrochem.* **38**, 669 (1932).
3. Schäfer, K., *Z. Elektrochem.* **64**, 1190 (1960).
4. Peters, C. L., Schäfer, K., and Krabetz, R., *Z. Elektrochem.* **64**, 1194 (1960).
5. Hosemann, R., Preisinger, A., and Vogel, W., *Ber. Bunsenges. Phys. Chem.* **70**, 796 (1966).
6. Brunauer, S., and Emmett, P. H., *J. Amer. Chem. Soc.* **62**, 1732 (1940).
7. Nielsen, A., "An Investigation on Promoted Iron Catalysts for the Synthesis of Ammonia." Jul. Gjellerups Forlag, Copenhagen, 1956.
8. Simmons, G., and Wang, H., "Single Crystal Elastic Constants and Calculated Aggregate Properties: A Handbook." M.I.T. Press, Cambridge, MA, 1971.
9. DiBenedetto, A. T., "The Structure and Properties of Materials." McGraw-Hill, New York, 1967.
10. Hirth, J. P., and Lothe, J., "Theory of Dislocations." McGraw-Hill, New York, 1968.